Application Note

Magnet Selection for Linear Position Applications

ABSTRACT

For position-sensing applications such as linear motor transport systems that must detect the position of a magnet sliding along a linear path, the geometry of the magnet and its relative air gap to the sensor will influence the behavior of the magnetic field as the magnet passes by the sensor.

Additionally, it is important in any system to maximize the sensing range for each sensor to reduce component count and save cost. In smaller applications that require only a low quantity of sensors, often the cost of the single magnet may overwhelm the total cost of the sensors. However, it may be worthwhile to consider the use of a slightly larger magnet to reduce the total number of sensors in large arrays.

This application note will discuss the placement, calibration, and sensing range of various magnet geometries and materials with 3D magnetic sensors, like the TMAG5170 and TMAG5273, in linear arrays.

Table of Contents

Trademarks

1 Introduction

When detecting the linear motion of a magnet in any system, it is important to maximize the total sensing range of the sensor for a particular magnet in use while maintaining a tight tolerance on overall measured position error. This allows the designer to minimize the size of the magnet and reduce the total number of Hall-effect sensors needed in an array to capture the full stroke length of the system.

Tighter tolerances for magnetic position sensing will produce improved feedback in controlled systems like linear motor transport systems by providing exact locations for each individual mover in the system. In linear motor transport systems, there are typically several individual movers that drive around a track or platform using repeating linear motors. For any mover, it is important to understand absolute position at all times to properly place the target at each manufacturing step, to efficiently move the platforms for maximum throughput, and to accurately drive the motor stage controlling that position.

Traditionally, this function has been supported by one-dimensional linear Hall-effect sensors, such as the DRV5055 which capture the z-component of the magnetic field when using the SOT-23 package.

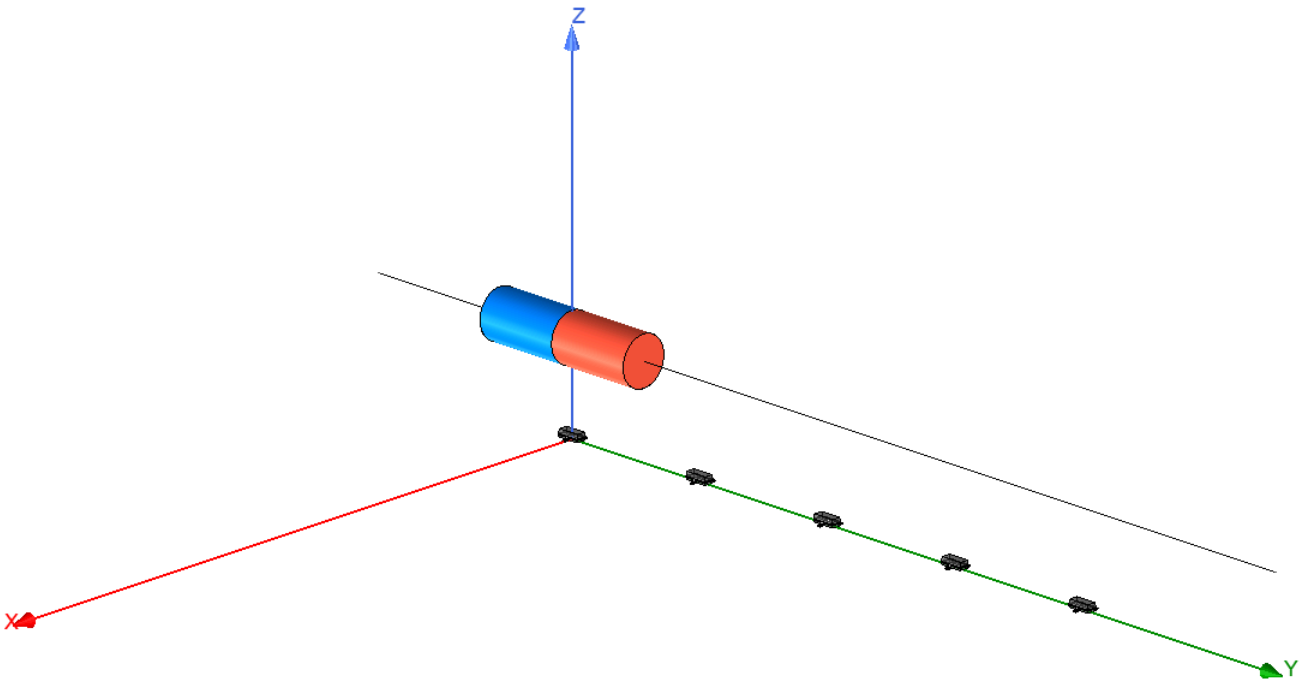

Figure 1-1. Linear Position Sense Array With One-Dimensional Hall-Effect Sensors

In this style of position-sensing configuration, the sensing range is limited to a linear region of the input magnetic field which is approximately the length of the magnet.

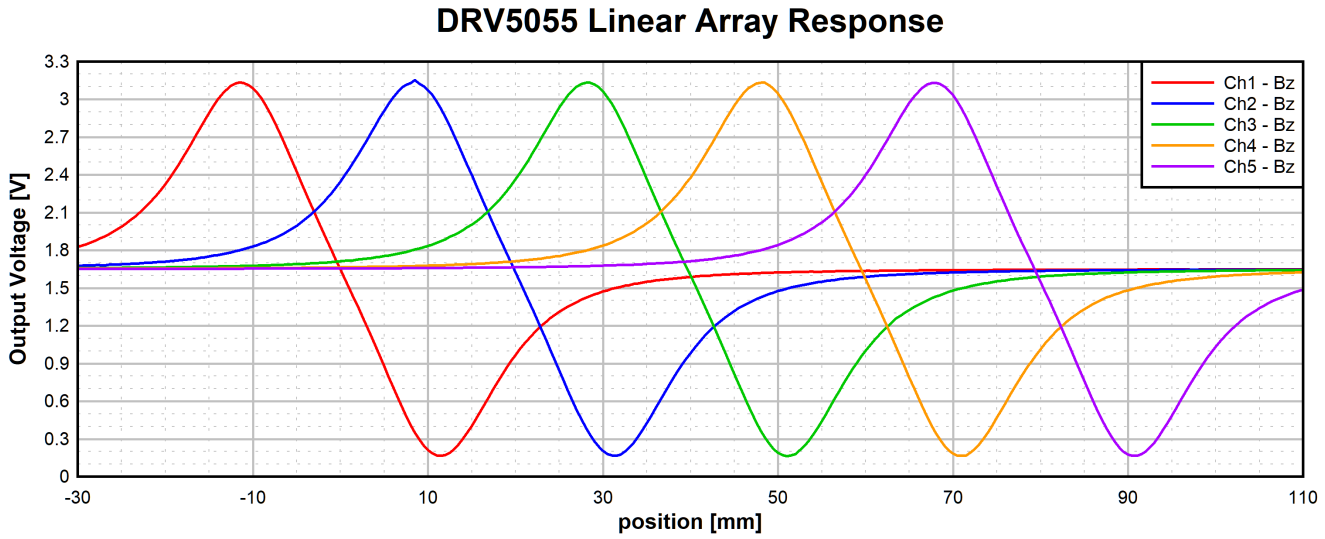

Figure 1-2. DRV5055 Output in Linear Array Configuration

This configuration is described in more detail in Linear Hall Effect Sensor Array Design.

There are significant advantages gained by implementing this solution using a 3D linear Hall-effect sensor like the TMAG5170 or TMAG5273. Firstly, the sensors are capable of detecting each component of the complete B-field vector. With expanded information, it is possible to identify exact magnet position over a range of motion longer stroke lengths than could be detected using a single axis sensor. Additionally, these sensors have integrated functions for amplitude and offset correction which are useful for correcting various electro-mechanical factors.

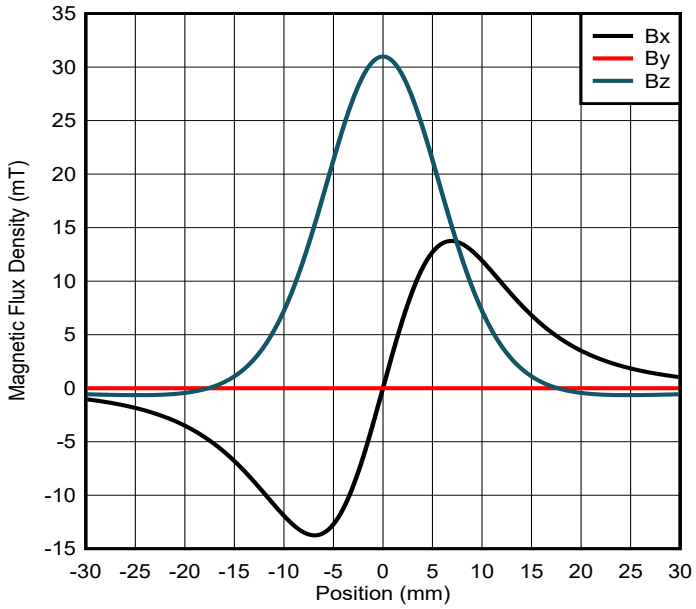

Figure 1-3. Example Magnetic Field Components Observed During Linear Motion

It is worthwhile then to examine how the selection of a magnet will impact the quality of the position measurement in a slide-by arrangement using a 3D sensor, and how to best linearize this measurement for minimal error.

2 Magnet Selection

Impact of Magnet Parameters

When selecting a magnet for a linear mover, it is important to consider temperature, magnetic material, magnet grade, magnet geometry, and general mechanical constraints. These system variables all have an impact on the overall function and reliability of the system.

As an example study, an axially magnetized cylinder magnet with a remanence (B_r) of 850 mT was simulated traveling above a sensor with an incrementally increased air gap.

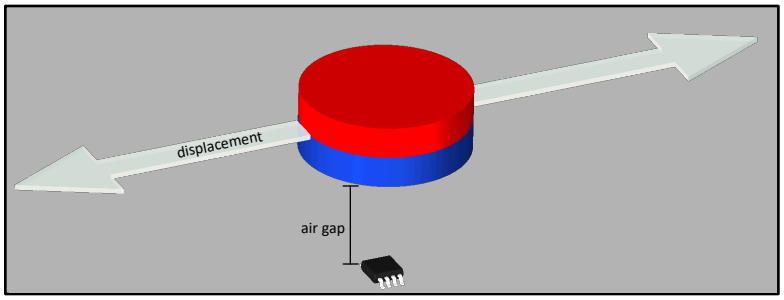

Figure 2-1. Slide-By Linear Magnetic Position Sensing

The magnet had an outer diameter of 16 mm and a thickness of 6 mm. Each horizontal line represents the magnitude of the vertical component (B_z) of the observable magnetic flux density. Plotted together, a 3D heat map is produced that shows how this one field component varies in the region below the magnet. In this case, the horizontal displacement is swept from –40 mm to +40 mm, and the vertical air gap between the sensor and magnet ranges from 2 mm to 15 mm.

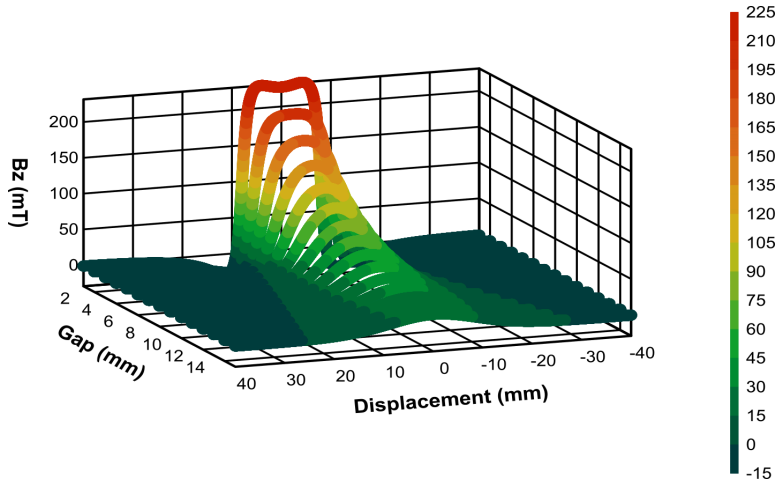

Figure 2-2. B-Field Z Component vs Linear Position

In the case of TMAG5170, the device offers two variants, each with three user programmable input ranges that vary from ±25 mT to ±300 mT. Any inputs above the maximum range will not be useful.

When examining these results closely, it is noticeable that when the air gap distance between the sensor element and magnet is very small, there is distortion near the peak of the bell-shaped input curve as it begins to flatten. At very close ranges, non-ideal peaking results from the corner effects of the magnet body concentrating on the magnetic field.

For comparison, consider how a change in the magnet geometry can impact overall function. For instance, if the magnet had an outer diameter of 8 mm while all other parameters were the same, you could note several different changes in behavior.

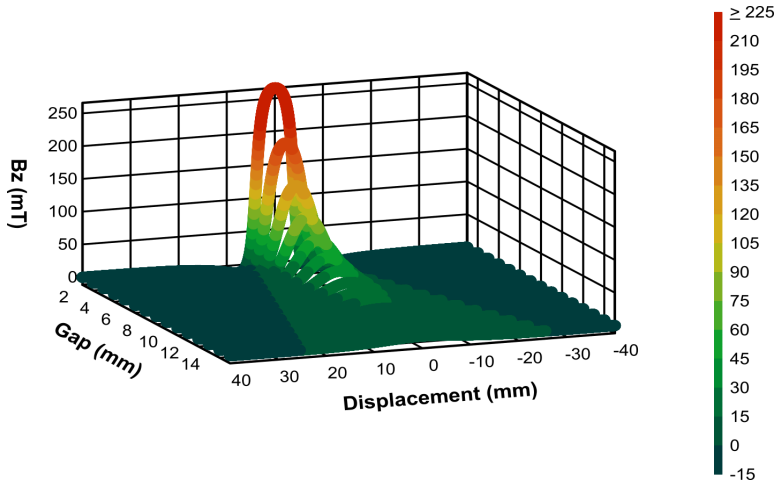

Figure 2-3. Linear Position Sweep With Reduced Magnet Diameter

One noted change is that the useful width of the input range dramatically reduced. The Calibration Method section explains that the maximum sensing range will typically be at least 2x the diameter of the magnet.

Additionally, the corner effects observed at very close proximity are dramatically reduced when using a narrower magnet. It is also apparent that the peak amplitude drops quickly when the air gap range increases. Intuitively, the sensing range for a smaller magnet is not as large as the sensing range of the original. What makes things even more difficult is that reducing the signal-to-noise ratio (SNR) will increase uncertainty in any measurement. It is therefore ideal to target a peak input value nearly the full scale input range of the sensor selected.

Assuming then that the larger diameter is more desirable for the increased sensing range, another study of the impact of the magnet thickness will be informative. Consider next, the impact of increasing the thickness from 6 mm to 12 mm.

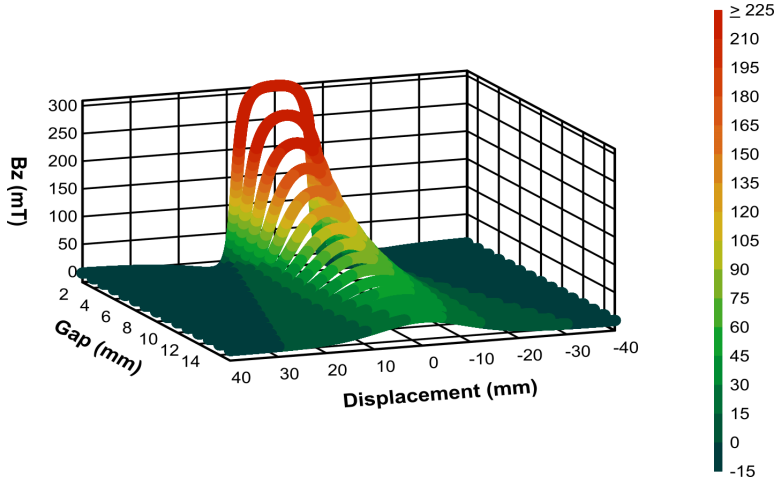

Figure 2-4. Linear Position Sweep With Increased Magnet Thickness

Similar to reducing the diameter of the magnet, increasing the thickness reduced the cornering effect, although visible distortion still occurs at very close proximity. From this, it is possible to deduce that the ratio of the thickness to the diameter will impact the closest sensing range possible for this motion. Unsurprisingly, the peak B-field magnitude also increased when a magnet with larger mass was used.

Beyond just the considerations for magnet size, the material and grade of the magnet can impact field strength and cost to build the system. For example, magnetic materials will weaken as temperatures rise. Table 2-1 shows the typical values for this behavior.

Table 2-1. Magnetic Material Temperature Response

Material	Temperature Drift (C)
NdFeB	-0.12%/C
SmCo	-0.04%/C
AlNiCo	-0.02%/C
Ferrite	-0.2%/C

If the working environment experiences large temperature variations, it may be beneficial to select a Samarium Cobalt (SmCo) magnet to reduce the effects of temperature drift.

It is also important to consider the approximate working air gap range for the sensor. The magnetic flux density observed by the sensor is inversely proportional to the square of the distance. That is, as the range increases, it is expected to see exponential decay in the strength of the field.

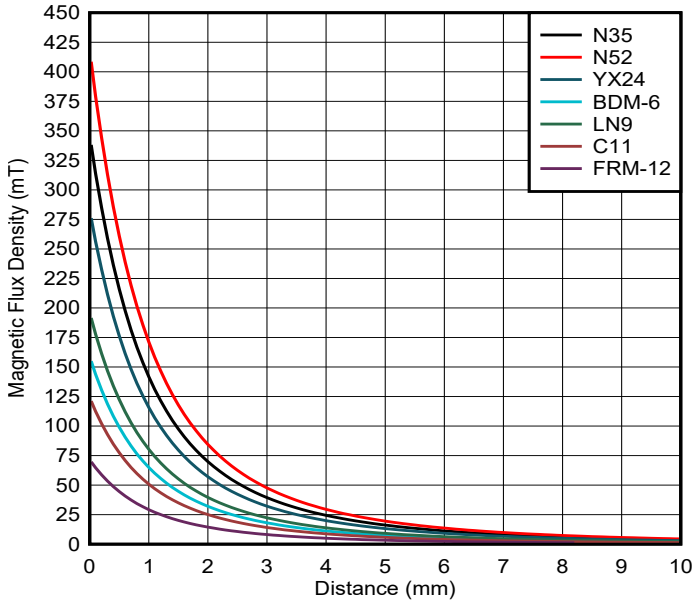

Figure 2-5. Magnetic Flux Density vs Air Gap Range for Various Magnet Materials

For any magnetic material, there are often several different grades of magnets which are usually distinguished by the B_r of the material. This value is well defined for any particular material, regardless of the size of the magnet. As B_r decreases, the B-field for any specific shape magnet will weaken. Neodymium type magnets, such as N35 and N52, tend to be the strongest commercially available option and inexpensive ferrite materials such as FRM-12 tend to be the weakest.

Calibration Method

For any particular magnet selected, the position of the magnet may be calculated by deriving the mechanical angle using the arctangent of the outputs of the Hall-effect sensor.

For example, the input field produced by Figure 2-6 with a remanence of 850 mT is shown in the following plot.

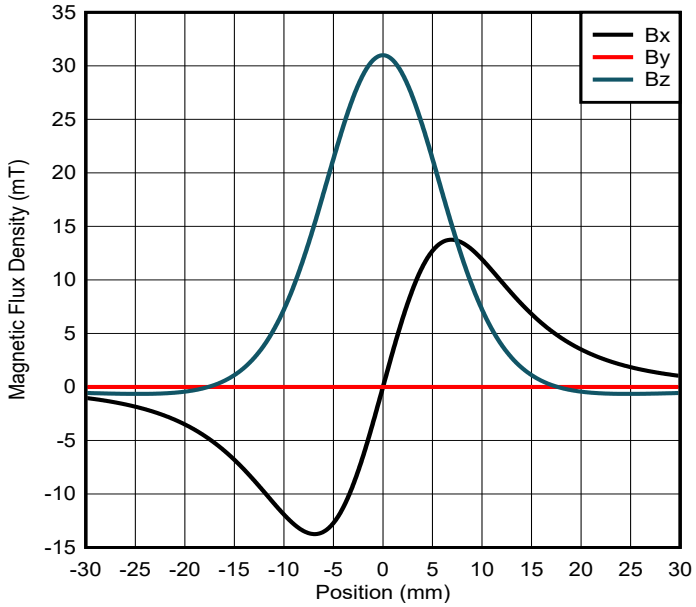

Figure 2-6. Magnet (10 mm ⌀ × 4 mm) at 10-mm Vertical Air Gap

Calculations of angle using these inputs directly can be compared to the real mechanical angle.

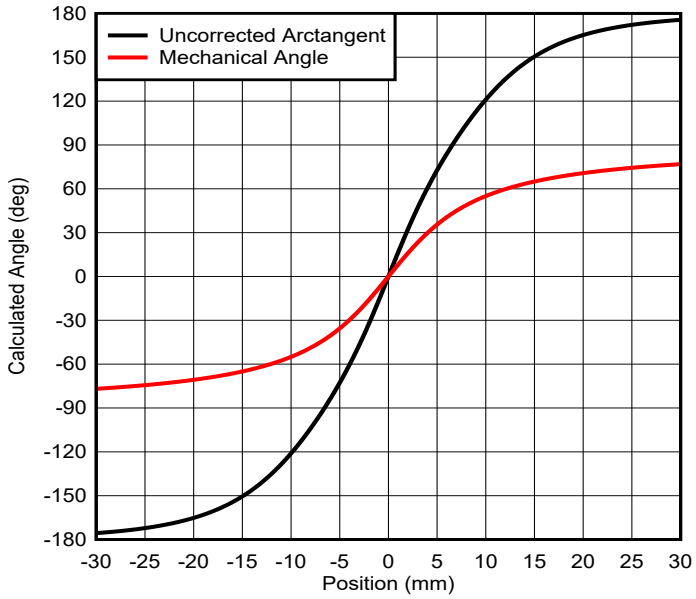

Figure 2-7. Mechanical Angle vs Calculated Arctangent

Notice that the form is similar but is distorted somewhat in shape and extent. This can be corrected using the following form:

$$Position = \tan\left(\gamma^{*}\text{atan}\left(\frac{\alpha^{*}(B_Z - \beta)}{B_X}\right) + \varphi^{*}B_X\right)^{*}\frac{magnet\ thickness + air gap}{2} \quad (1)$$

In Equation 1, four specific correction factors are required to obtain optimal linearity. **α** specifies the amplitude correction applied to the Z axis input, **β** specifies a fixed offset which must be applied to the Z axis input. **γ** is a scalar correction for the magnetic angle, and **φ** is a scalar factor of the Y axis input which corrects some non-linearity in the final result.

In this case, setting the following empirically derived values for each factor produce a final position accuracy shown in Figure 2-8.

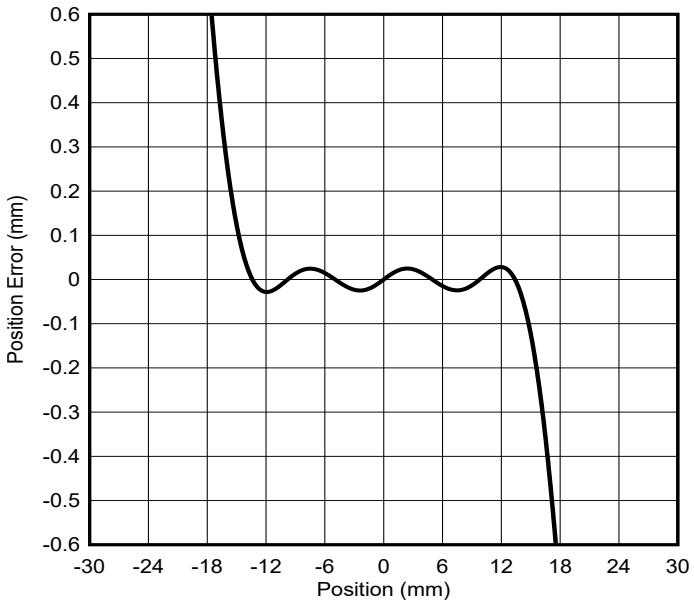

α = 0.791 ; **β** = 16.3 ; **γ** = 0.4104 ; **φ** = 0.448

Figure 2-8. Calibrated Position Error vs Absolute Position

This same method was applied in the following figures to obtain similar accuracy. In each case, the position error is minimized over a region **approximately 2x the diameter** of the magnet.

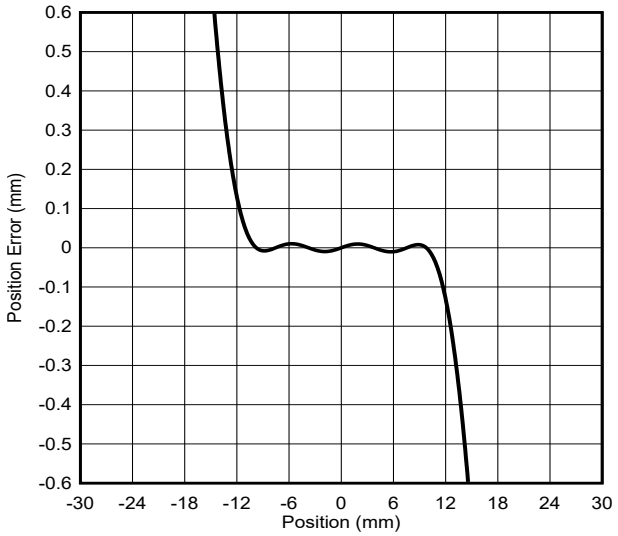

α = 0.833 ; **β** = 4.85 ; **γ** = 0.397 ; **φ** = 1.07

Figure 2-9. Position Error for Magnet (5 mm ⌀ × 4 mm) at 10-mm Air Gap

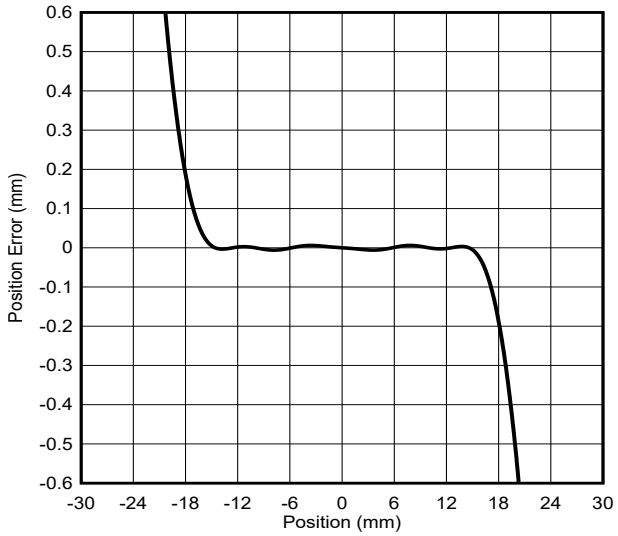

α = 0.739 ; **β** = 24.12 ; **γ** = 0.4215 ; **φ** = 0.4617

Figure 2-10. Position Error for Magnet (14 mm ⌀ × 4 mm) at 10-mm Air Gap

The quality of each calibration varies with the exactness of the correction factors applied. In the case of the largest diameter magnet, peak error in the sensing range is approximately 10 um.

Of similar note, the ratio of the potential sensing range to the magnet diameter is largest for the smaller (and weakest) magnet.

Similarly, it is possible to vary the air gap distance to demonstrate impact on the expected sensing range of the sensor. Consider the following plots based on the 14 mm ⌀ x 4mm magnet at air gaps of 5 mm and 20 mm.

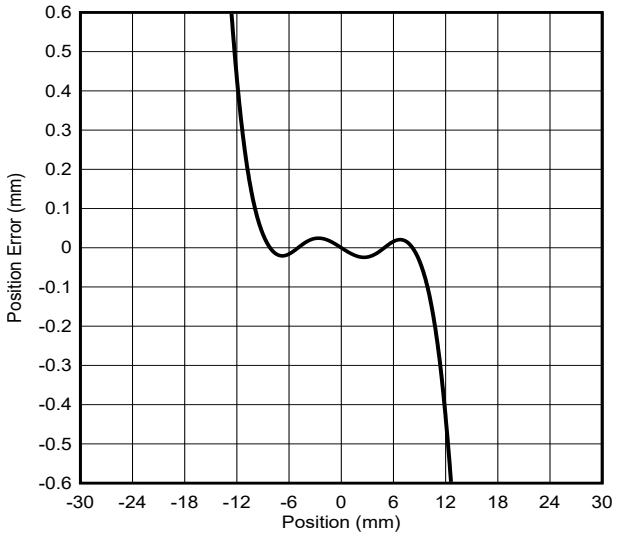

α = 0.79 ; **β** = 58.9 ; **γ** = 0.297 ; **φ** = 0.049

Figure 2-11. Position Error for Magnet (14 mm ⌀ × 4 mm) at 5-mm Air Gap

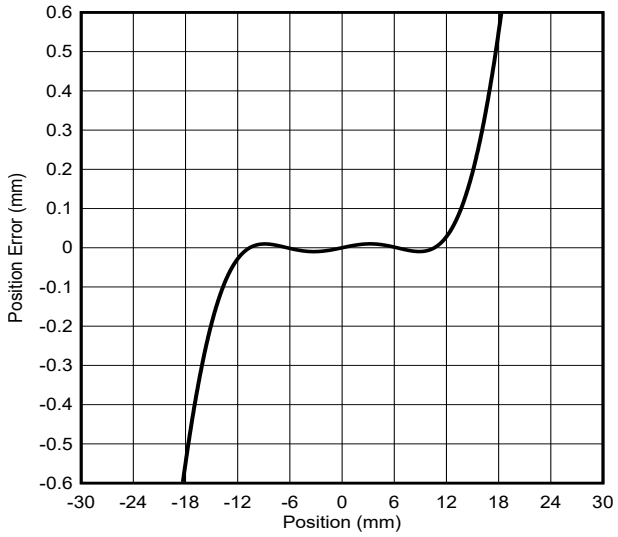

α = 0.775 ; **β** = 4.95 ; **γ** = 0.436 ; **φ** = 1.54

Figure 2-12. Position Error for Magnet (14 mm ⌀ × 4 mm) at 20-mm Air Gap

In both cases, the maximum sensing range for the magnet was reduced. In the case of the 5-mm air gap, the input field was limited by distortion. In the case of the 20-mm air gap, the sensing range is limited by the strength of the magnetic field. The design goal, therefore, is to target a strong magnetic field that neither saturates the input of the sensor nor becomes distorted due to close range of the magnet.

In some cases, it can be advantageous to use a bar-shaped magnet for ease of assembly. This calibration method is not limited to cylindrical magnets. Similar to the previous cases, implementing the same calibration method for a square-faced magnet traveling over the sensor will produce excellent linearity (see Figure 2-13).

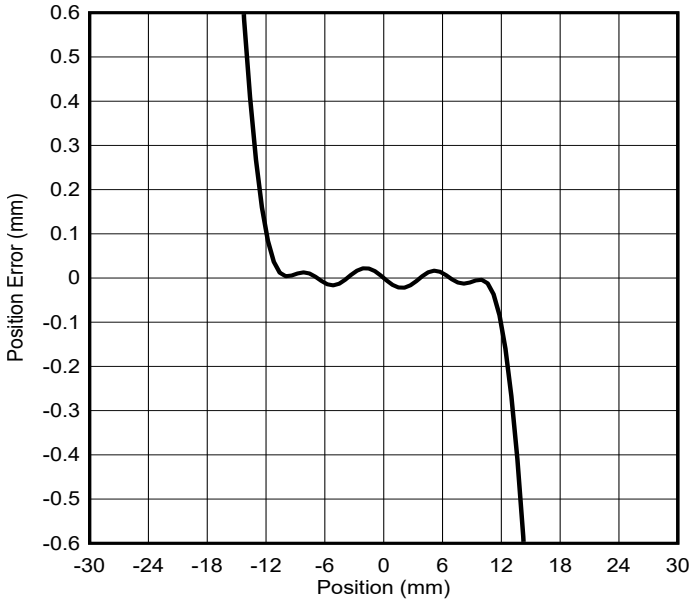

α = 0.75 ; **β** = 53.7 ; **γ** = 0.3815 ; **φ** = 0.089

Figure 2-13. Position Error for Magnet (10 mm × 10 mm × 4 mm) at 5-mm Air Gap

3 Summary

As was shown with the calibration results above, there are several options available to optimize the placement of each 3D Hall-effect sensor for long observable stroke distance. To ensure the highest quality results, a magnet which is strong enough to use most of the linear input range of the sensor is beneficial, and a wider magnet will produce a longer sensing range. It may also be beneficial in cases where air gap distance is minimized to use a thicker magnet to reduce distortion that may result near the corners of the magnet.

Implemented correctly, 3D Hall-effect sensors offer an increased sensing range by approximately 2x and as demonstrated in Figure 2-10 a linearity error of 10 µm is attainable. Maximizing the sensing range is critical to reducing the total number of sensors required in any linear position sensing application. Additionally, reducing linearity error is critical for precise control required for automated systems like linear motor transport systems to achieve quality and highly repeatable performance for manufacturing and assembly.

IMPORTANT NOTICE AND DISCLAIMER

TI PROVIDES TECHNICAL AND RELIABILITY DATA (INCLUDING DATA SHEETS), DESIGN RESOURCES (INCLUDING REFERENCE DESIGNS), APPLICATION OR OTHER DESIGN ADVICE, WEB TOOLS, SAFETY INFORMATION, AND OTHER RESOURCES “AS IS” AND WITH ALL FAULTS, AND DISCLAIMS ALL WARRANTIES, EXPRESS AND IMPLIED, INCLUDING WITHOUT LIMITATION ANY IMPLIED WARRANTIES OF MERCHANTABILITY, FITNESS FOR A PARTICULAR PURPOSE OR NON-INFRINGEMENT OF THIRD PARTY INTELLECTUAL PROPERTY RIGHTS.

These resources are intended for skilled developers designing with TI products. You are solely responsible for (1) selecting the appropriate TI products for your application, (2) designing, validating and testing your application, and (3) ensuring your application meets applicable standards, and any other safety, security, regulatory or other requirements.

These resources are subject to change without notice. TI grants you permission to use these resources only for development of an application that uses the TI products described in the resource. Other reproduction and display of these resources is prohibited. No license is granted to any other TI intellectual property right or to any third party intellectual property right. TI disclaims responsibility for, and you will fully indemnify TI and its representatives against, any claims, damages, costs, losses, and liabilities arising out of your use of these resources.

TI’s products are provided subject to TI’s Terms of Sale or other applicable terms available either on ti.com or provided in conjunction with such TI products. TI’s provision of these resources does not expand or otherwise alter TI’s applicable warranties or warranty disclaimers for TI products.

TI objects to and rejects any additional or different terms you may have proposed.

Mailing Address: Texas Instruments, Post Office Box 655303, Dallas, Texas 75265